

# JGR Biogeosciences

## RESEARCH ARTICLE

10.1029/2020JG005793

### Key Points:

- Temperature, daylength, and light intensity influenced methane production from marine algae
- Light intensity showed a very pronounced effect on methane formation rates from all investigated species
- Global change will likely increase methane release rates of marine phytoplankton

### Supporting Information:

- Supporting Information S1

### Correspondence to:

T. Klintzsch and F. Keppler,  
thomas.klintzsch@geow.uni-heidelberg.de;  
frank.keppler@geow.uni-heidelberg.de

### Citation:




Klintzsch, T., Langer, G., Wieland, A., Geisinger, H., Lenhart, K., Nehrke, G., & Keppler, F. (2020). Effects of temperature and light on methane production of widespread marine phytoplankton. *Journal of Geophysical Research: Biogeosciences*, 125, e2020JG005793. <https://doi.org/10.1029/2020JG005793>

Received 22 APR 2020

Accepted 6 AUG 2020

Accepted article online 25 AUG 2020

## Effects of Temperature and Light on Methane Production of Widespread Marine Phytoplankton

T. Klintzsch<sup>1</sup> , G. Langer<sup>2</sup> , A. Wieland<sup>1</sup>, H. Geisinger<sup>1</sup>, K. Lenhart<sup>1,3</sup>, G. Nehrke<sup>4</sup>, and F. Keppler<sup>1,5</sup> 

<sup>1</sup>Institute of Earth Sciences, University Heidelberg, Heidelberg, Germany, <sup>2</sup>The Laboratory, Citadel Hill, The Marine Biological Association of the United Kingdom, Plymouth, UK, <sup>3</sup>Professorship of Botany, Limnology and Ecotoxicology, University of Applied Sciences, Bingen, Germany, <sup>4</sup>Marine Biogeosciences, Alfred Wegener Institut – Helmholtz-Zentrum für Polar- und Meeresforschung, Bremerhaven, Germany, <sup>5</sup>Heidelberg Center for the Environment HCE, Heidelberg University, Heidelberg, Germany

**Abstract** Methane (CH<sub>4</sub>) production in the ocean surface mixed layer is a widespread but still largely unexplained phenomenon. In this context marine algae have recently been described as a possible source of CH<sub>4</sub> in surface waters. In the present study we investigated the effects of temperature and light intensity (including daylength) on CH<sub>4</sub> formation from three widespread marine algal species *Emiliania huxleyi*, *Phaeocystis globosa*, and *Chrysochromulina* sp. Rates of *E. huxleyi* increased by 210% when temperature increased in a range from 10°C to 21.5°C, while a further increase in temperature (up to 23.8°C) showed reduction of CH<sub>4</sub> production rates. Our results clearly showed that CH<sub>4</sub> formation of *E. huxleyi* is controlled by light: When light intensity increased from 30 to 2,670 μmol m<sup>-2</sup> s<sup>-1</sup>, CH<sub>4</sub> emission rates increased continuously by almost 1 order of magnitude and was more than 1 order of magnitude higher when the daylength (light period) was extended from 6/18 hr light-dark cycle to continuous light. Furthermore, light intensity is also an important factor controlling CH<sub>4</sub> emissions of *Chrysochromulina* sp. and *P. globosa* and could therefore be a species-independent regulator of phytoplankton CH<sub>4</sub> production. Based on our results, we might conclude that extensive blooms of *E. huxleyi* could act as a main regional source of CH<sub>4</sub> in surface water, since blooming of *E. huxleyi* is related to the seasonal increase in both light and temperature, which also stimulate CH<sub>4</sub> production. Under typical global change scenarios, *E. huxleyi* will increase its CH<sub>4</sub> production in the future.

**Plain Language Summary** Methane is a gas that affects the Earth's climate and is typically produced by microbes in the absence of oxygen or through geological processes. Surprisingly, methane is also produced in oceanic surface waters that are well oxygenated, known as the ocean-methane paradox. Marine phytoplankton has recently been discovered as a methane source, which might help to explain the paradox. Environmental factors such as light and temperature might be important for controlling methane production from marine algae. In order to understand how environmental factors affect methane formation from phytoplankton, we performed several experiments under laboratory conditions. We find that temperature, light intensity, and day length strongly control methane production of phytoplankton. The field blooms of marine algae, which are often strongly related to the seasonal increase of light and temperature, could act as an important regional source of methane in oceanic surface waters. Under typical global change scenarios, marine algae might increase their methane production in the 21st century.

## 1. Introduction

Huge amounts of methane (CH<sub>4</sub>) are formed in the oceans, but only a small proportion is released to the atmosphere (Weber et al., 2019). In this context the biogeochemical cycle of CH<sub>4</sub> in the oceans is of great interest, and in particular, the frequently observed CH<sub>4</sub> production within the ocean surface mixed layer is challenging our previous understanding of biogeochemical CH<sub>4</sub> formation processes. Traditionally, it is thought that CH<sub>4</sub> in the oceans is either produced by geological processes (abiotic) or by methanogenic archaea (biotic). Because methanogenic archaea are strict anaerobic microorganism, their CH<sub>4</sub> production is limited to anoxic environments (Kirschke et al., 2013; Saunio et al., 2016; Thauer et al., 2008). However, there is growing evidence that CH<sub>4</sub> is also produced by organisms such as cyanobacteria (Bižić et al., 2020) and eukaryotes including plants (Keppler et al., 2006), fungi (Lenhart et al., 2012), lichens

©2020. The Authors.

This is an open access article under the terms of the Creative Commons Attribution License, which permits use, distribution and reproduction in any medium, provided the original work is properly cited.

(Lenhart et al., 2015) and algae (Klitzsch et al., 2019; Lenhart et al., 2016), animals (Ghyczy et al., 2008), and humans (Keppler et al., 2016) and even in the presence of oxygen.

The observation of CH<sub>4</sub> in freshwater and saline surface waters (often described as methane paradox) has recently received much attention although some studies already conducted four decades ago (Scranton, 1977; Scranton & Brewer, 1977; Scranton & Farrington, 1977) have reported about CH<sub>4</sub> supersaturation in the ocean mixed layer. Furthermore, many recent studies (Grossart et al., 2011; Günthel et al., 2019; Hartmann et al., 2020; Tang et al., 2016) have shown that CH<sub>4</sub> formation is not limited to salt-water but also occurs in freshwater lakes. Several hypotheses exist to explain CH<sub>4</sub> formation in oxygenated waters, and some of them will be discussed briefly. Methanogenic archaea living in anoxic environments of particles or fish and zooplankton guts might form CH<sub>4</sub> (de Angelis & Lee, 1994; Karl & Tilbrook, 1994; Schmale et al., 2018; Stawiariski et al., 2019; Zindler et al., 2013). The algal methabolite dimethylsulfoniopropionate (DMSP) and its degradation products dimethyl sulfide (DMS) or dimethyl sulfoxide (DMSO) could be precursors of both archaeal (Damm et al., 2008; Florez-Leiva et al., 2013) and bacterial produced CH<sub>4</sub>, when bacteria suffer under nitrogen deficiency (Damm et al., 2010). Moreover, photochemical degradation of DMS and acetone has been shown to produce CH<sub>4</sub>, but the reaction is limited to anoxic waters (Bange & Uher, 2005; Zhang, Xie, et al., 2015). In oligotrophic Pacific waters CH<sub>4</sub> formation might mainly related to the bacterial cleavage of methylphosphonates when supply of phosphorous is limited (del Valle & Karl, 2014; Karl et al., 2008; Metcalf et al., 2012; Repeta et al., 2016).

Phytoplankton might contribute to CH<sub>4</sub> production in both oxic marine and freshwater environments. The first indication of CH<sub>4</sub> production from phytoplankton was provided by culture experiments of the diatom species *Thalassiosira pseudonana* and the haptophyte species *E. huxleyi* (Scranton, 1977; Scranton & Brewer, 1977; Scranton & Farrington, 1977). Later on, many field studies have reported a relationship between CH<sub>4</sub> supersaturation and the occurrence of phytoplankton in lakes and oceans (e.g., Bogard et al., 2014; Conrad & Seiler, 1988; Damm et al., 2008; Grossart et al., 2011; Oudot et al., 2002; Owens et al., 1991; Rakowski et al., 2015; Tang et al., 2014; Weller et al., 2013; Zindler et al., 2013). Although a good statistical correlation was not observed in all previous studies (e.g., Brooks et al., 1981; Burke et al., 1983; Forster et al., 2009; Lamontagne et al., 1975; Watanabe et al., 1995), it was suggested that phytoplankton is one of the likely CH<sub>4</sub> sources. However, clear evidence of CH<sub>4</sub> formation from marine algae—examined in cultures of marine haptophytes—was only provided recently when Lenhart et al. (2016) and Klitzsch et al. (2019) applied stable isotope labeling experiments to unambiguously show that the three widespread marine algae such as *E. huxleyi*, *Chrysochromulina* sp., and *Phaeocystis globosa* indeed produce CH<sub>4</sub> per se and without the help of methanogenic archaea. Very recently, when using stable isotope labeling experiments and concentration measurements, it could be also shown that several freshwater algal species, including diatoms, cryptophytes, and green algae (Hartmann et al., 2020), but also several species of marine and limnic cyanobacteria (Bižić et al., 2020) emit CH<sub>4</sub>. Thus, both marine algae and cyanobacteria could significantly contribute to the commonly observed oceanic CH<sub>4</sub> supersaturation (Bižić et al., 2020; Klitzsch et al., 2019; Scranton, 1977). In summary, previous investigations mainly focused on explaining the sources for CH<sub>4</sub> in oxic surface waters; however, the effects of environmental parameters such as temperature, light intensity, or nutrient availability on CH<sub>4</sub> production from phytoplankton are still unknown.

In the present study we investigated the effects of temperature and light intensity (including daylength) on CH<sub>4</sub> formation from the three widespread marine algal species *E. huxleyi*, *P. globosa*, and *Chrysochromulina* sp. *Emiliania huxleyi* occurs in ocean worldwide except in the polar regions (McIntyre et al., 1970). The algal species develops large populations (blooms) in subpolar to temperate areas usually in summer time, especially under highly stratified conditions, when the mixed layer depth shallows due to increasing temperature. Blooming of *E. huxleyi* is then supported by high light intensity caused by shallow mixed layer depth and incidence light (Nanninga & Tyrrell, 1996; Raitos et al., 2006; Tyrrell & Merico, 2004; Tyrrell & Taylor, 1996). Therefore, we have studied in detail CH<sub>4</sub> formation in relation to temperature (range from 10.1°C to 23.8°C), light intensity (30 to 2,670 μmol m<sup>-2</sup> s<sup>-1</sup>), and daylength (period of light irradiation) during growth of *E. huxleyi*. We furthermore investigated the effect of light intensity on CH<sub>4</sub> formation by the two other widespread marine, but noncalcifying haptophytes *P. globosa* and *Chrysochromulina* sp. These two species can also form large blooms and are often found as main members in marine phytoplankton communities (Brown & Yoder, 1994; Schoemann et al., 2005; Thomsen, 1994). The results of *E. huxleyi* will be

discussed with regard to their potential importance in marine environments during blooming. Finally, the observed CH<sub>4</sub> formation patterns of the three algal species will be evaluated on the basis of the CH<sub>4</sub> production potential (CH<sub>4</sub>-PP), which expresses differences in growth rates and thus the success of a species at the community level.

## 2. Materials and Methods

### 2.1. Experimental Setup

*Emiliania huxleyi* RCC1216 provided from the Roscoff Culture Collection (<http://roscoff-culture-collection.org/>, last access: 11 April 2020) were used to investigate the effect of temperature, light intensity, and day-length on CH<sub>4</sub> production rates. We performed an additional experiment to study the effect of light intensity on different algae species. Therefore, *E. huxleyi* and two other haptophytes *P. globosa* PLY 575 and *Chrysochromulina* sp. PLY 307 obtained from the Marine Biological Association of the United Kingdom (<https://www.mba.ac.uk/facilities/culture-collection>, last access: 11 April 2020) were studied. The cultures were maintained in quasi-exponential growth by frequent dilution with medium in order to keep them largely free of bacteria. All culture experiments were conducted under the use of sterile techniques. For a more detailed discussion about the potential interplay between algae and bacteria, we would like to refer the reader to the manuscript by Klintzsch et al. (2019). Briefly, Klintzsch et al. concluded that CH<sub>4</sub> production is clearly dependent on algal growth and that it is highly unlikely that bacteria alone are responsible for CH<sub>4</sub> production in the studied cultures. Each sample was taken at the end of the light period. Cultures were grown in batch mode (Langer et al., 2013). We used F/2 growth medium (Guillard & Ryther, 1962) that was based on sterile filtered (0.2 μm Ø pore size) North Sea seawater (sampled off Helgoland, Germany, 32 PSU). Cells were grown in crimped serum bottles (160 ml) filled with 140 ml medium and 20 ml headspace. Culture experiments were carried out with four independent repetitions. For determination of the CH<sub>4</sub> mixing ratio samples of 10 ml of headspace gas was sampled. The amount of produced CH<sub>4</sub> in culture group vials was calculated in respect to control groups. The culture and control group flasks were simultaneously sealed under ambient air and thus contained the same CH<sub>4</sub> background concentration. Please note that the produced CH<sub>4</sub> has been determined for the entire incubation flask—dissolved in the medium plus CH<sub>4</sub> of the headspace volume. For details on determination of CH<sub>4</sub> formation, please refer to section 2.2. For all experiments performed with algae and F/2 medium, the average CH<sub>4</sub> content in the cultures group at the end of incubation was higher than that found in the algae-free blanks as shown in Tables S1–S4. All growth rates and initial and final cell densities are given in the supporting information (Tables S1–S4).

Cultures were illuminated by cold white LED bulbs (LED Base Classic A100, Osram, Germany). The light spectrum of the LED bulbs is provided in Figure S1. The photosynthetic active radiation (PAR) was measured inside each incubation jar by using a light meter (ULM-500 Universal, WALZ, Germany) with a spherical quantum PAR sensor (US-SQS/L, WALZ, Germany). Temperature was logged by (UX120-006 M, HOBO, Germany).

### 2.2. Determination of CH<sub>4</sub> Mass

The CH<sub>4</sub> mass was determined at the end of the incubation period. In order to determine the CH<sub>4</sub> mass of the whole incubation flask (dissolved plus the CH<sub>4</sub> of the headspace volume), an aliquot (10 ml) of head space gas was taken from the incubation vials using a gastight syringe. In order to maintain headspace pressure when taking the headspace gas sample, an equivalent volume of seawater was injected into the flasks by syringe. The added volume was taken into account when determining the cell density (section 2.5). The sample gas was separated by gas chromatography using a GC-14B (Shimadzu, Japan) equipped with a 2 m column (Ø = 3.175 mm inner diameter), packed with Molecular Sieve 5A 60/80 mesh from Supelco. Methane was recorded by a flame ionization detector (FID) and quantified (mixing ratio) by using two reference standards containing 9,837 and 2,192 parts per billion by volume (p.p.b.v) CH<sub>4</sub>. Mixing ratios were corrected for head space pressure. The latter was measured inside the incubation flask before gas sampling using a pressure meter (GMSD 1,3 BA, Greisinger). The CH<sub>4</sub> mass ( $m_{\text{CH}_4}$ ) was determined by its mixing ratio ( $x_{\text{CH}_4}$ ) and the ideal gas law (Equation 1),

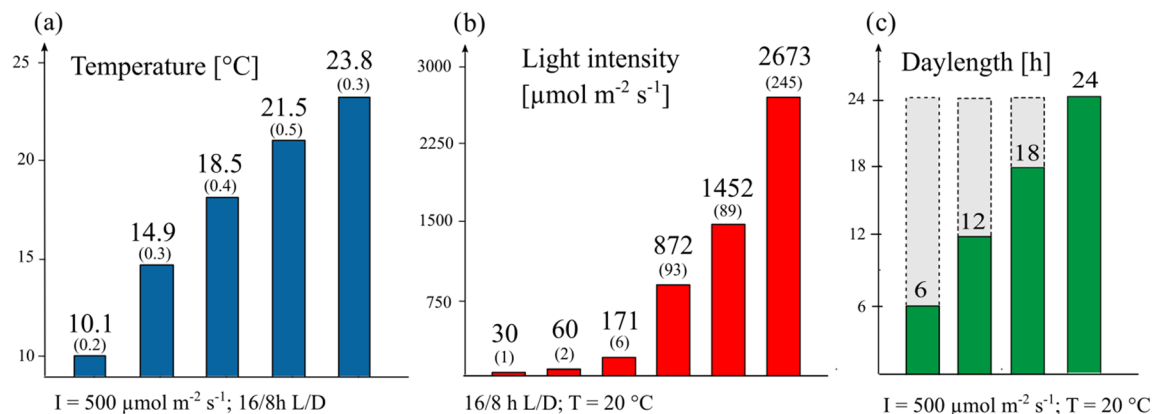


**Figure 1.** Treatment conditions of temperature (a), light intensity (b), and daylength (c) experiment. All treatments were carried out with four independent replications. L/D = light/dark; I = light intensity. (a) Mean values of logged temperature during the test period. (b) Mean light intensity values that were measured inside each incubation jar. The standard deviation is given in brackets.

$$m_{CH_4} = M_{CH_4} \times x_{CH_4} \frac{p \times V}{R \times T}, \quad (1)$$

where  $M_{CH_4}$  = molar mass,  $p$  = pressure,  $T$  = temperature,  $R$  = ideal gas constant, and  $V$  = volume.

The dissolved  $CH_4$  concentration was calculated by using the equation of Wiesenburg and Guinasso (1979).

### 2.3. Treatments of Alternating Temperature, Light Intensity, or Daylength at Cultures of *E. huxleyi*

To investigate the effect of temperature, light intensity, and daylength (daylength refers to the light period within a 24-hr light-dark cycle), three independent experiments with *E. huxleyi* were carried out in which one of the three parameters was varied as described in Figure 1. Within each experiment, the other two parameters were kept constant with 16/8-hr light-dark cycle;  $\sim 500 \mu\text{mol photons m}^{-2} \text{s}^{-1}$  and  $20^\circ\text{C}$ , respectively. All treatments were carried out with four independent repetitions. Control groups contained F/2 medium only. Cultures were acclimated ( $\approx 10$  generations) to the environmental conditions prior to the experiment. Cell density at inoculation varied between treatments depending on the growth rates under the given environmental conditions. Cultures of *E. huxleyi* were allowed to grow not more than  $0.4 \times 10^6 \text{ cells ml}^{-1}$  (exponential phase) before they were harvested. The majority ( $>95\%$ ) of culture replicates reached final cell densities between  $0.1 \times 10^6$  and  $0.3 \times 10^6 \text{ cells ml}^{-1}$  (Tables S1–S3). Possible culture artifacts of  $CH_4$  production rates, which could result from a cell density effect (Langer et al., 2013), were excluded for each investigated parameter by correlating the  $CH_4$  production rates with the cell density on the harvest day (Figure S2).

### 2.4. Treatments of Alternating, Light Intensity on Cultures of *P. globosa*, *Chrysochromulina* Sp., and *E. huxleyi*

The effect of light intensity was studied in two further haptophytes: *P. globosa* and *Chrysochromulina* sp. in addition to *E. huxleyi*. Two light intensities ( $427 \pm 12 \mu\text{mol m}^{-2} \text{s}^{-1}$  and  $1,165 \pm 42 \mu\text{mol m}^{-2} \text{s}^{-1}$ ) with four replicates were applied, respectively. Cultures were grown under a 16/8 hr light-dark cycle and  $20^\circ\text{C}$ . Cultures were preadapted ( $\approx 10$  generations) to light intensities before the experiment was started. The initial and final cell densities correspond to the exponential phase for each species (Klintzsch et al., 2019) and are given in the supporting information (Table S4). Control groups contained F/2 medium only.

### 2.5. Determination of Cell Density

For the determination of cell densities either a Fuschs-Rosenthal or Neubauer counting chamber (depending on cell density) was used. At least minimum of four aliquots of each culture sample were counted.

## 2.6. Determination of Growth and CH<sub>4</sub> Production Rates

All production rates were measured at exponentially growing cultures. For further information of measuring production rates from batch culture experiments, we refer to Klintzsch et al. (2019) and Langer et al. (2012, 2013).

We calculated the growth rate ( $\mu$ ) from cell densities ( $N$ ) of the beginning ( $t_0$ ,  $N_0$ ) and end ( $t_1$ ,  $N_1$ ) of the experiment (Equation 2).

$$\mu = \frac{\ln(N_1) - \ln(N_0)}{(t_1 - t_0)} \quad (2)$$

The POC-based CH<sub>4</sub> production rates were calculated from the cellular organic carbon content ( $POC_{cell}$ ). The latter was obtained from cell volume ( $V_{cell}$ ) by using the carbon to volume relationship in Equation 3 according to Menden-Deuer and Lessard (2000):

$$POC_{cell} = 0.216 \times V_{cell}^{0.939}. \quad (3)$$

The cell volume was calculated from the cell diameter in light micrographs, which was measured by using the program ImageJ (Schindelin et al., 2012). We followed the recommendation of Olenina et al. (2006) and assumed a ball shape for calculating the cell volume for the three species investigated here.

The carbon-specific growth rate was calculated from the product of POC and growth rate  $\mu$  (Equation 4):

$$\mu_{POC} = \mu \times POC_{cell}. \quad (4)$$

The CH<sub>4</sub> production rates were calculated by multiplying the growth rate  $\mu$  with the corresponding cellular or POC-CH<sub>4</sub> quota, which was measured at the end of the experiment. The daily cellular CH<sub>4</sub> production rates ( $CH_4P_{cell}$ ,  $\mu\text{g CH}_4 \text{ cell}^{-1} \text{ day}^{-1}$ ,  $\mu\text{g} = 10^{-18} \text{ g}$ ) were calculated according to Equation 5:

$$CH_4P_{cell} = \mu \times \frac{m(CH_4)}{cell}, \quad (5)$$

where  $m(CH_4)$  is the amount of CH<sub>4</sub> that was produced at the end of the experiment.

The daily cellular CH<sub>4</sub> production rates ( $CH_4P_{POC}$ ,  $\mu\text{g CH}_4 \text{ g}^{-1} \text{ POC day}^{-1}$ ) were calculated from growth rate and CH<sub>4</sub>-POC quotas at the end of the experiment according to Equation 6.

$$CH_4P_{POC} = \mu \times \frac{m(CH_4)}{POC}. \quad (6)$$

The CH<sub>4</sub> production potential (CH<sub>4</sub>-PP) was calculated to scale variations in cellular production rates to community level. Detailed explanations for calculating the production potential (PP, which is not confined to CH<sub>4</sub>) have been provided by Gafar et al. (2018) and Gafar and Schulz (2018). Please note that these authors have calculated the PP for CaCO<sub>3</sub> but the concept is the same for CH<sub>4</sub>. In accordance to the authors, the CH<sub>4</sub>-PP can be calculated for different growth periods, when a cellular standing stock for each time period is calculated from a given starting cell density ( $N_0$ ). The related amount of produced CH<sub>4</sub> (CH<sub>4</sub>-PP) for each period of growth and respectively standing stock is the product of the cellular standing stock and CH<sub>4</sub> quota (Equation 7).

$$CH_4PP = N_0 \times e^{\mu \times t} \times \frac{m(CH_4)}{cell} \quad (7)$$

In the present study and in accordance to Klintzsch et al. (2019) the CH<sub>4</sub>-PP was calculated for a standing stock that is obtained after 7 days of growth starting with a single cell.

The sensitivity of growth, POC production and the rate of CH<sub>4</sub> formation to temperature were quantified by their activation energy ( $E_a$ ), which is derived from the Arrhenius equation (Equation 8).

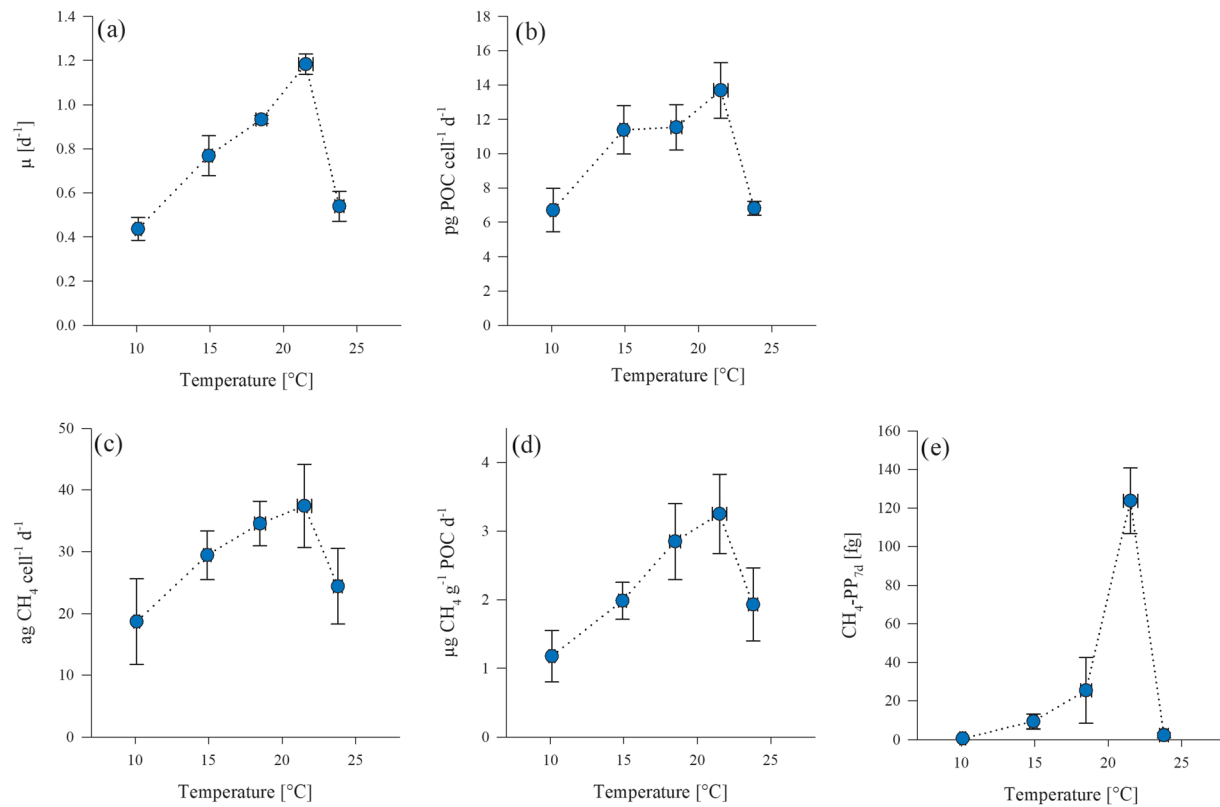


**Figure 2.** Relationship between temperature and growth rate (a), POC production rate (b), cellular (c), and POC normalized CH<sub>4</sub> production rate (d) and CH<sub>4</sub>-PP (e) of *E. huxleyi*. Values are the mean of four replicated culture experiments with standard deviation (SD).

$$k(T) = A_{exp} \left( \frac{-E_a}{RT} \right), \quad (8)$$

where  $k$  = reaction rate constant (here for growth, POC, or CH<sub>4</sub> production rate),  $A$  = pre-exponential factor,  $R$  = gas constant, and  $T$  = temperature. The activation energies ( $E_a$ ) of the rate can then be calculated by multiply the slope of the Arrhenius plot by  $-R$ , using a plot of  $\ln(k)$  as function of  $T^{-1}$ .

## 2.7. Statistics

For each environmental factor (sections 3.1–3.3) the total data set of cellular and POC normalized CH<sub>4</sub> production was analyzed for statistical differences in the mean values among the treatment groups by using a one-way analysis of variance (ANOVA). Furthermore, within the individual culture experiments of *E. huxleyi*, *P. globosa*, and *Chrysochromulina* sp. (section 3.4), the mean values (cellular and POC normalized CH<sub>4</sub> production) of the two light intensities treatments (medium and high light) were compared by  $t$  tests.

## 3. Results

### 3.1. Temperature Effect

Growth and POC production rates have more than doubled when increasing temperatures from 10.5°C to 21.5°C (Figures 2a and 2b). The optimum of growth and POC production was reached at 21.5°C (1.18 day<sup>-1</sup>; 13.7 ± 1.6 pg POC cell<sup>-1</sup> day<sup>-1</sup>), while a further increase in temperature to 23.8°C led to a drastic reduction of about 50% for both growth and POC production rates. A similar pattern was observed for CH<sub>4</sub> production rates (cellular and POC normalized) as shown in Figures 2c and 2d. The POC normalized and cellular CH<sub>4</sub> production increased by 2.8- and 2.0-fold, respectively, when temperature increased by 11.4°C (from 10.1°C to 21.5°C). At 21.5°C the optimum of CH<sub>4</sub> production rates was reached (3.2 ± 0.6 μg CH<sub>4</sub> g<sup>-1</sup> POC day<sup>-1</sup>; 37.4 ± 6.7 ag CH<sub>4</sub> cell<sup>-1</sup> day<sup>-1</sup>). Further increase in temperature from 21.5°C to 23.8°C

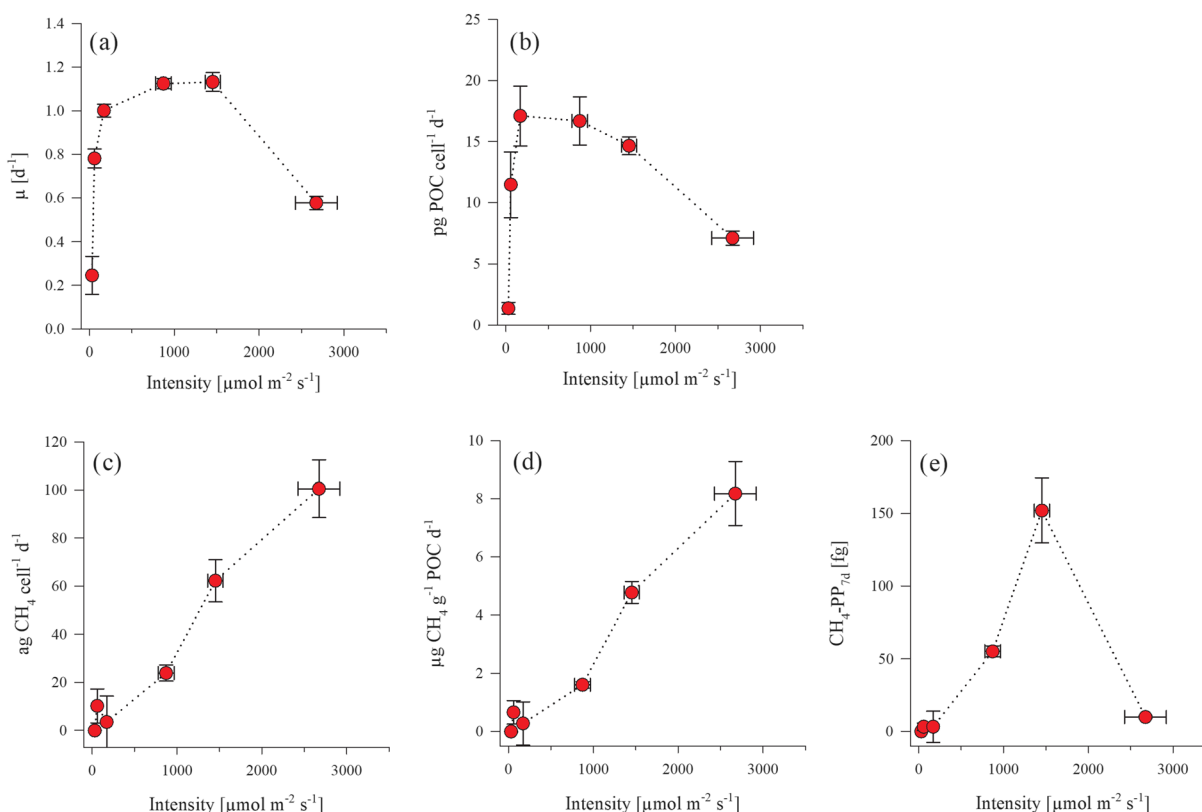


**Figure 3.** Relationship between light intensity and growth rate (a), POC production rate (b), cellular (c), and POC normalized CH<sub>4</sub> production rate (d) and CH<sub>4</sub>-PP e of *E. huxleyi*. Values are the mean of four replicated culture experiments with SD.

showed a reduction of CH<sub>4</sub> production by 40% and 35%, for POC normalized and cellular CH<sub>4</sub> production, respectively. Statistical analysis (ANOVA) confirmed the temperature dependence of CH<sub>4</sub> production with *p* values of 0.002 and <0.001 for POC normalized and cellular CH<sub>4</sub> production rates, respectively. After 1 week of growth the total amount of generated CH<sub>4</sub> is specified by the CH<sub>4</sub>-PP (Figure 2e). With increasing temperature (from 10.1°C to 21.5°C) the CH<sub>4</sub>-PP raised by 2 orders of magnitude (from  $0.7 \pm 0.2$  to  $124 \pm 17.1$  fg CH<sub>4</sub>) before it declined drastically at 23.8°C (Figure 2e). Consequently, the optimum temperature (21.5°C) was identical for the five investigated parameters (Figure 2).

### 3.2. Light Intensity Effect

The growth and POC production rates of *E. huxleyi* increased drastically when light intensity increased from 30 to  $171 \mu\text{mol m}^{-2} \text{s}^{-1}$ , and values remained relatively constant at higher light intensities in the range of  $171$ – $1,450 \mu\text{mol m}^{-2} \text{s}^{-1}$  (Figures 3a and 3b). However, increasing the light intensity to  $2,670 \mu\text{mol m}^{-2} \text{s}^{-1}$  caused a clear reduction of both growth and POC production rates. From 30 to  $171 \mu\text{mol m}^{-2} \text{s}^{-1}$  the growth rate increased fourfold (from  $0.25 \pm 0.09$  to  $1.00 \pm 0.03 \text{ day}^{-1}$ ) and POC production rates by over 1 order of magnitude (from  $1.4 \pm 0.48$  to  $17.1 \pm 2.5 \text{ pg POC cell}^{-1} \text{ day}^{-1}$ ). The POC production was highest at  $171 \mu\text{mol m}^{-2} \text{s}^{-1}$  and was similar at  $872 \mu\text{mol m}^{-2} \text{s}^{-1}$  while rates were slightly smaller at  $1,452 \mu\text{mol m}^{-2} \text{s}^{-1}$ . The growth rate increased by 10% between 171 and  $872 \mu\text{mol m}^{-2} \text{s}^{-1}$  but did not further change when reaching values of  $1,450 \mu\text{mol m}^{-2} \text{s}^{-1}$  ( $1.13 \pm 0.03 \text{ day}^{-1}$ ). Thus, the optimum growth rate is reached at higher light intensities compared to the POC production rates. However, a further increase in light intensity up to  $2,673 \mu\text{mol m}^{-2} \text{s}^{-1}$  led to a significant reduction ( $\approx 45\%$ ) of both POC production and growth rates. In contrast, the cellular and POC normalized CH<sub>4</sub> production rates increased steadily with increasing light intensity (Figures 3c and 3d). Methane formation (on a cell basis) was below the detection limit at  $30 \mu\text{mol m}^{-2} \text{s}^{-1}$  but measurable ( $6.9 \pm 9.5 \text{ ag CH}_4 \text{ cell}^{-1} \text{ day}^{-1}$ ;  $0.47 \pm 0.63 \text{ pg POC cell}^{-1} \text{ day}^{-1}$  on average) between 60 and  $171 \mu\text{mol m}^{-2} \text{s}^{-1}$  while at  $872 \mu\text{mol m}^{-2} \text{s}^{-1}$  production rates strongly increased ( $23.9 \pm 3.3 \text{ ag CH}_4 \text{ cell}^{-1}$

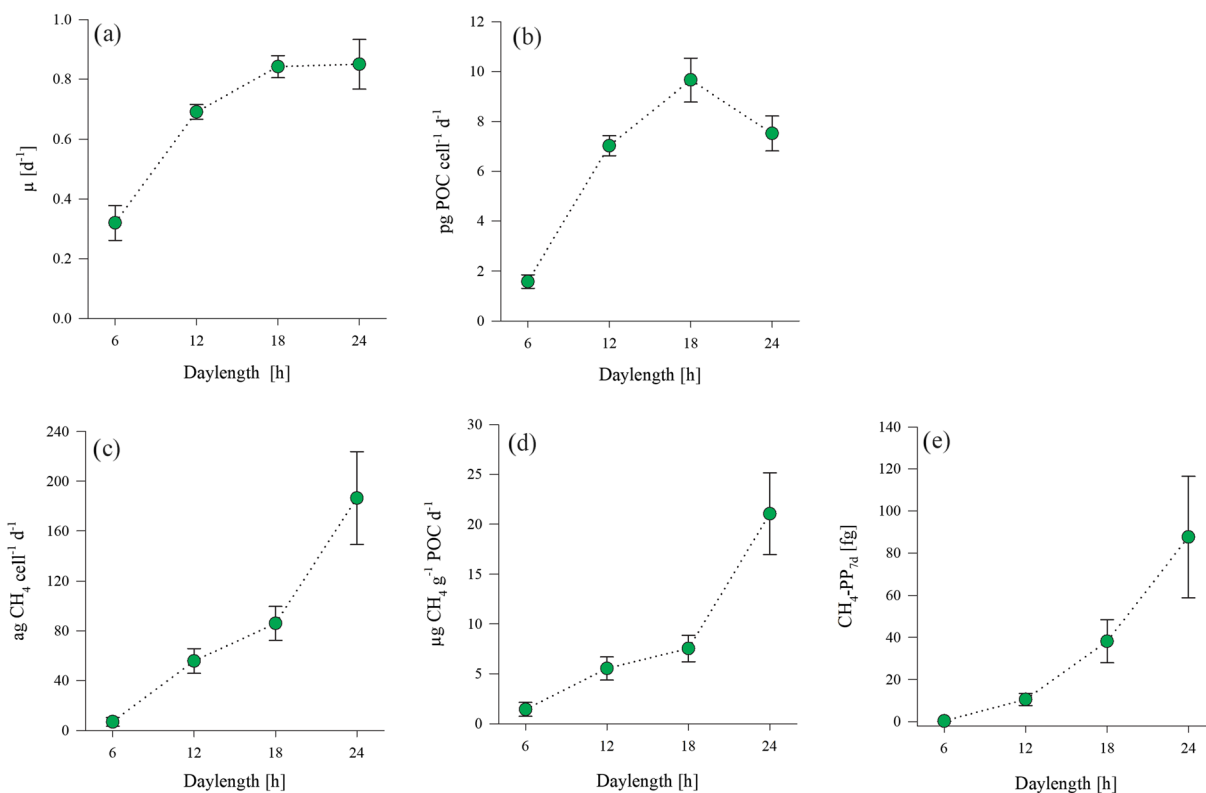


**Figure 4.** Relationship between day length and growth rate (a), POC production rate (b), cellular (c), and POC normalized CH<sub>4</sub> production rate (d) and CH<sub>4</sub>-PP (e) of *E. huxleyi*. Values are the mean of four replicated culture experiments with SD.

day<sup>-1</sup>;  $1.6 \pm 0.1 \mu\text{g CH}_4 \text{ g}^{-1} \text{ POC day}^{-1}$ ). From 872 to  $2,670 \mu\text{mol m}^{-2} \text{ s}^{-1}$  cellular and POC normalized CH<sub>4</sub> production increased by 4.2- and 5.1-fold up to  $100 \pm 12 \text{ ag CH}_4 \text{ cell}^{-1} \text{ day}^{-1}$  and  $6.8 \pm 0.9 \mu\text{g CH}_4 \text{ g}^{-1} \text{ POC day}^{-1}$ , respectively. The light dependence of both cellular and POC-normalized CH<sub>4</sub> production was also indicated by statistical analysis (ANOVA;  $p < 0.001$ ). The CH<sub>4</sub>-PP (Figure 3e) increased with increasing light intensities by 2 orders of magnitude up to  $152 \pm 22 \text{ fg CH}_4$  at  $1450 \mu\text{mol m}^{-2} \text{ s}^{-1}$  and sharply decreased by one order of magnitude (to  $9.9 \pm 0.9 \text{ fg CH}_4$ ) at higher light intensity ( $2,670 \mu\text{mol m}^{-2} \text{ s}^{-1}$ ). The optimum of CH<sub>4</sub>-PP is therefore in accordance with the optimum of growth rate.

### 3.3. Daylength Effect

The extension of the daylength (period of light irradiation) from 6 to 18 hr increased the growth rates 2.6-fold (from  $0.32 \pm 0.06$  to  $0.84 \pm 0.04 \text{ day}^{-1}$ ), while the growth rates remained constant when a period of continuous light (24 hr) was set (Figure 4a). In contrast to the growth rate, an optimum of POC production rates was observed at 18 hr daylength and decreasing with longer irradiation period of 24 hr (Figure 4b). POC production rates increased between 6 and 18 hr daylength by 6.1-fold (from  $1.6 \pm 0.3$  to  $9.7 \pm 0.9 \text{ pg POC cell}^{-1} \text{ day}^{-1}$ ) and declined by 22% at continuous light. Cellular and POC normalized CH<sub>4</sub> production rates increased from 6 hr daylength to continuous light period by 2 and 1 order of magnitude from  $6.9 \pm 3.4$  to  $186 \pm 37 \text{ ag CH}_4 \text{ cell}^{-1} \text{ day}^{-1}$  and  $1.1 \pm 0.6$  to  $21.0 \pm 4.1 \mu\text{g CH}_4 \text{ g POC}^{-1} \text{ day}^{-1}$ , respectively (Figures 4c and 4d). The dependence of CH<sub>4</sub> production on temperature was verified by statistical analysis (ANOVA), with cellular and POC normalized CH<sub>4</sub> production rates showing  $p$  values of  $p < 0.001$  and  $p = 0.004$ , respectively. The cellular and POC normalized CH<sub>4</sub> production was particularly enhanced by the 6 hr extension of the daylength between 18 hr and continuous light that accounted for 56% and 69% of the total increase in cellular and POC normalized CH<sub>4</sub> production, correspondingly. The CH<sub>4</sub>-PP increased constantly by over 2 orders of magnitude with longer light irradiation periods (from  $0.19 \pm 0.12 \text{ fg CH}_4$  at 6 hr light to  $70.4 \pm 23.1 \text{ fg CH}_4$  at continuous light, Figure 4e).

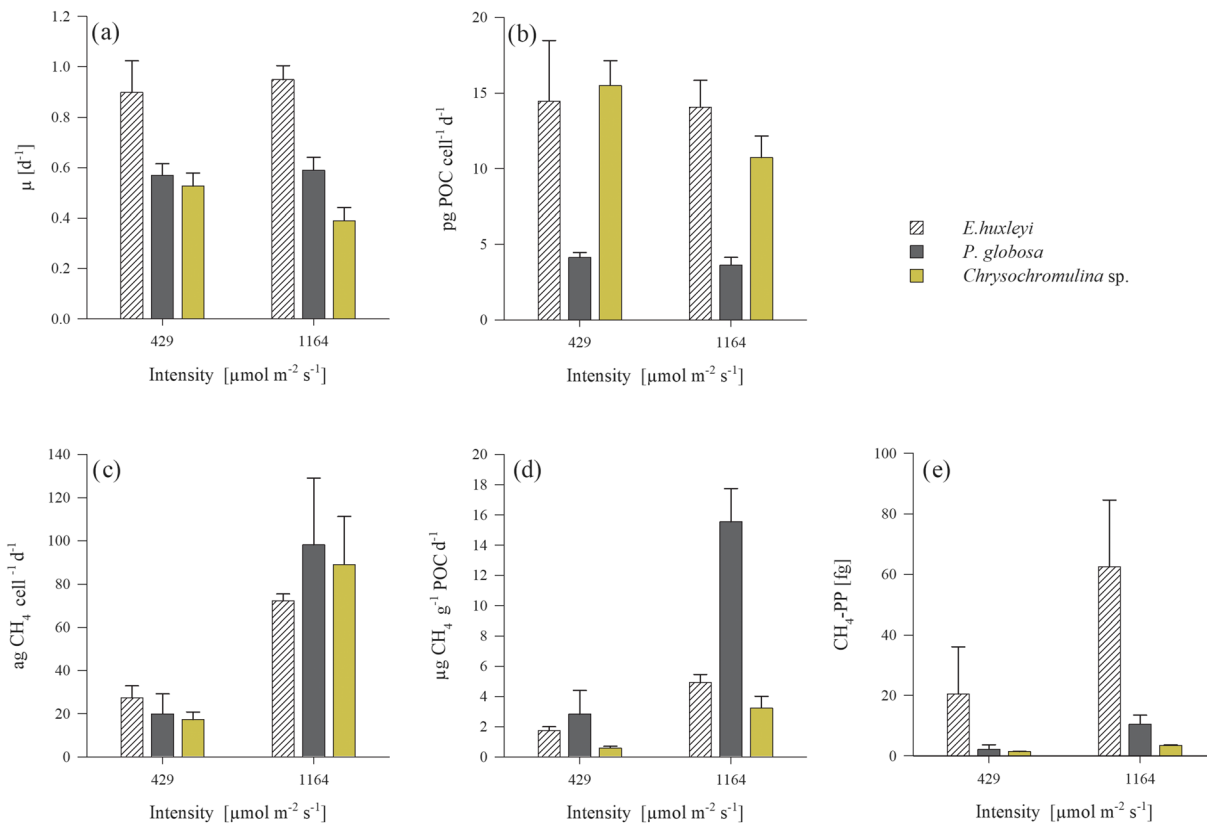


**Figure 5.** Relationship between light intensity and growth rate (a), POC production rate (b), cellular (c), and POC normalized  $\text{CH}_4$  production rate (d) and  $\text{CH}_4$ -PP (e) of *E. huxleyi*, *P. globosa*, and *Chrysochromulina* sp. by moderate ( $429 \mu\text{mol m}^{-2} \text{s}^{-1}$ ) and high light intensity ( $1,164 \mu\text{mol m}^{-2} \text{s}^{-1}$ ). Values are the mean of four replicated culture experiments with SD.

### 3.4. Comparison of Light Intensity Effects of *E. huxleyi*, *Chrysochromulina* Sp., and *P. globosa*

We compared growth and  $\text{CH}_4$  formation patterns of the three algal species *E. huxleyi*, *P. globosa*, and *Chrysochromulina* sp. at moderate and high light intensities ( $429 \mu\text{mol m}^{-2} \text{s}^{-1}$  and  $1,164 \mu\text{mol m}^{-2} \text{s}^{-1}$ ). The growth rates at both light intensities are shown in Figure 5a. At moderate light intensity the exponential growth rate  $\mu$  was highest for *E. huxleyi* ( $0.90 \pm 0.13 \text{ day}^{-1}$ ) followed by *P. globosa* and *Chrysochromulina* sp. (with  $0.57 \pm 0.05 \text{ day}^{-1}$  and  $0.55 \pm 0.04 \text{ day}^{-1}$ , respectively). Growth rates of *E. huxleyi* and *P. globosa* remained constant at higher intensity, while growth rate of *Chrysochromulina* sp. declined by 29%. The POC production rates are shown in Figure 5b. At moderate light intensity the POC production rates of *E. huxleyi* and *Chrysochromulina* sp. were in the same range with  $14.5 \pm 0.5$  and  $15.5 \pm 1.6 \text{ pg POC cell}^{-1} \text{ day}^{-1}$ , respectively, and were about three times higher than for *P. globosa* ( $4.1 \pm 0.3 \text{ pg POC cell}^{-1} \text{ day}^{-1}$ ). The exposure to high light intensity led to a 31% lower POC production rate of *Chrysochromulina* sp. while rates of *E. huxleyi* and *P. globosa* remained constant. Thus, an increase in light intensity declined growth rate and POC production of *Chrysochromulina* sp., while that of *E. huxleyi* and *P. globosa* remained constant. Cellular  $\text{CH}_4$  production rates of all investigated species were enhanced by increasing light intensities (Figure 5c). Cellular  $\text{CH}_4$  production rates ranged from  $17 \pm 3.6$  (*Chrysochromulina* sp.) to  $27 \pm 5.6 \text{ ag CH}_4 \text{ cell}^{-1} \text{ day}^{-1}$  (*E. huxleyi*) at medium light. In response to higher light intensity the cellular  $\text{CH}_4$  production rates increased by 2.6-fold (*E. huxleyi*) and about fivefold (*P. globosa* and *Chrysochromulina* sp.) resulting in a cellular  $\text{CH}_4$  production rates ranged from  $72.1 \pm 3.3$  (*E. huxleyi*) to  $98.2 \pm 30.8 \text{ ag CH}_4 \text{ cell}^{-1} \text{ day}^{-1}$  (*P. globosa*). The response in cellular production rates to higher light intensity was also displayed by *t* test with *p* values of  $<0.001$ ,  $0.006$ , and  $0.005$  for *E. huxleyi*, *P. globosa*, and *Chrysochromulina* sp., respectively. The POC normalized  $\text{CH}_4$  production rates increased with increasing light intensity (Figure 5d). Within the medium and high light intensities, the variation of POC normalized  $\text{CH}_4$  production rates between

species was greater than that of cellular CH<sub>4</sub> production rates. When CH<sub>4</sub> production rates were normalized to POC, rates of moderate light intensities were in a range of  $0.58 \pm 0.12$  to  $2.8 \pm 1.6 \mu\text{g CH}_4 \text{ g}^{-1} \text{ POC day}^{-1}$  with *Chrysochromulina* sp. and *P. globosa* showing the lowest and highest rates, respectively. At high light intensity rates were about 2.8-fold (*E. huxleyi*) and 5.5-fold (*P. globosa* and *Chrysochromulina* sp.) greater than for those observed at moderate light intensity. These differences were also shown by *t* test with *p* values <0.001, 0.004, and <0.001 for *E. huxleyi*, *P. globosa*, and *Chrysochromulina* sp., respectively. The respective rates ranged from  $3.24 \pm 0.78$  (*Chrysochromulina* sp.) to  $15.6 \pm 2.2 \mu\text{g CH}_4 \text{ g}^{-1} \text{ POC day}^{-1}$  (*P. globosa*). All three species showed enhanced CH<sub>4</sub>-PP with the higher light intensity (Figure 5e). The increase from moderate to high light ranged between 2.4-fold (*Chrysochromulina* sp.) and 4.9-fold (*P. globosa*). However, the variation of the CH<sub>4</sub>-PP within the species is greater than that resulting from the different light treatments. The CH<sub>4</sub>-PP was 1 order of magnitude higher for *E. huxleyi* in comparison to the other two species (Figure 5e). This is in line with the higher growth rate of *E. huxleyi*.

## 4. Discussion

Previous studies indicated that several marine algae produce CH<sub>4</sub> (Klitzsch et al., 2019; Lenhart et al., 2016; Scranton, 1977; Scranton & Brewer, 1977; Scranton & Farrington, 1977), while the modulating influence of environmental parameters is unknown. Our results clearly show that CH<sub>4</sub> formation by *E. huxleyi* is influenced by temperature, light intensity, and the length of irradiation period. Furthermore, light intensity is also an important factor controlling emission rates of the two other marine algae *Chrysochromulina* sp. and *P. globosa*. We will first discuss the effects of environmental parameters on growth and POC normalized CH<sub>4</sub> production from a physiological perspective. Afterward, the effects of environmental parameters on laboratory CH<sub>4</sub> production rates of *E. huxleyi* are discussed in relation to their possible importance on populations (blooms) in marine environments. Finally, we discuss the impact of environmental parameters on CH<sub>4</sub> production in biogeochemical terms using the well-established but rarely applied concept of the PP (see Klitzsch et al., 2019, and references therein).

### 4.1. Temperature Effect on Growth and CH<sub>4</sub> Formation of *E. huxleyi* From a Physiological Perspective

*Emiliania huxleyi* occurs, except for the polar regions, in oceans worldwide and has the largest known temperature growth range (1–31°C) compared to other coccolithophores (McIntyre et al., 1970). The temperature response of growth rate is strain specific (Brand, 1982; Langer et al., 2009), and the optimum temperature for strain RCC1216 in this study tallies well with the published value (Langer et al., 2009). The growth curve (Figure 2a) exhibits the asymmetry typical for a temperature response. The ascending, shallow sloped, part of the curve is characterized by an accelerating effect of temperature on all biochemical reactions, whereas the descending, steep sloped, part is characterized by inactivation of enzymes, and denaturation of proteins and membranes (DeLong et al., 2017; Grimaud et al., 2017; Kingsolver, 2009). In accordance with this general concept of temperature effects on physiological processes, we observe a positive correlation of all analyzed physiological parameters with temperature up to 21.5°C (the optimum) followed by a negative correlation above this temperature. We conclude that CH<sub>4</sub> production is a normal physiological process as opposed to a heat stress response stemming from structural damage to cellular architecture. Please note that CH<sub>4</sub> production trends are identical, regardless of the normalization, that is, normalization to cell or POC (Figures 2c and 2d).

The ascending part of the temperature curve can be further analyzed using the Arrhenius equation. According to this equation (Equation 8), the thermal sensitivity of a chemical reaction is proportional to its activation energy. While the Arrhenius equation was originally used to describe chemical reactions, the equation might be also applied to describe the thermal sensitivity of biochemical reactions and biological growth rates, whereby high activation energies indicate high sensitivity to temperature (Gillooly et al., 2001; Grimaud et al., 2017). The calculated activation energies of growth rate, POC, and CH<sub>4</sub> production were 59, 41, and 63 kJ mol<sup>−1</sup>, respectively. The growth rate and CH<sub>4</sub> production are therefore somewhat more sensitive to temperature than POC production is. The activation energy of CH<sub>4</sub> production is in the range of basic metabolic processes, indicating that CH<sub>4</sub> production in algae is not an abiotic process. For example, the average activation energy of respiration for a wide range of organisms, including microbes, plants, and animals,

is between 40 and 71 kJ mol<sup>-1</sup> (Gillooly et al., 2001). In addition, activation energies of most enzymatic reactions are in the range of 21 to 63 kJ mol<sup>-1</sup> (Segel, 1993). By contrast abiotic CH<sub>4</sub> formation from thermal degradation experiments as described from dried soils usually showed higher activation energies above 70 kJ mol<sup>-1</sup> (Jugold et al., 2012; Liu et al., 2019).

## 4.2. Light Intensity and Daylength Effects on Growth and CH<sub>4</sub> Formation of *E. huxleyi* From a Physiological Perspective

We grew *E. huxleyi* under a wide range of light intensities and daylengths.

### 4.2.1. Light Intensity

Our results demonstrate that CH<sub>4</sub> formation and growth rate of *E. huxleyi* is sensitive to light intensity. Under light-limited condition, growth rate increased sharply with increasing light intensity, leveled off at saturated light, and decreased at inhibiting light intensities (Figures 3a and 3b). This pattern of light intensity response (Figure 3a) is typical of phytoplankton cultures (Edwards et al., 2015, and reference inside). The optimum light intensity for POC production is lower than the one for growth rate, which was also observed by Trimborn et al. (2007). The growth rate of *E. huxleyi* was remarkably tolerant against high light intensities ( $\geq 1,500 \mu\text{mol m}^{-2} \text{s}^{-1}$ ), a phenomenon well documented in the literature (Balch et al., 1992; Gafar & Schulz, 2018; Harris et al., 2005; Loebl et al., 2010; Nanninga & Tyrrell, 1996; Nielsen, 1997; Trimborn et al., 2007). Interestingly CH<sub>4</sub> production was even more tolerant to high light, so much so that we could not determine the optimum light intensity. This is in notable contrast to the temperature response patterns described above. While we do not know the chain of events leading to this light intensity response, the response patterns suggest that, first, CH<sub>4</sub> production is a light dependent process and, second, photo-inhibition of growth rate and POC production do not impair CH<sub>4</sub> production. The latter is particularly intriguing because it seems to suggest a decoupling of CH<sub>4</sub> production from photosynthetic production of both energy equivalents and putative CH<sub>4</sub> precursors originating in the POC pool. This warrants further, more detailed, physiological studies into the nature of the light dependency of CH<sub>4</sub> production.

### 4.2.2. Daylength

The CH<sub>4</sub> formation and growth rate were furthermore controlled by daylength. The growth rate showed a saturation curve (Figure 4a). This pattern is similar to results on *E. huxleyi* reported by Paasche (1967) and even other phytoplankton species (e.g., Bouterfas et al., 2006). By contrast, growth rates of *E. huxleyi* have been reported to be independent of daylength (Nielsen, 1997) or to be inhibited by continuous light (Van Rijssel & Gieskes, 2002). The response to daylength has been suggested to be strain specific (Bretherton et al., 2019) and is dependent on other environmental parameters, for example, on seawater CO<sub>2</sub> concentration (Bretherton et al., 2019; Zhang, Bach, et al., 2015) and light quality (Glover et al., 1987). This could be one reason why the response of growth in relation to daylength differs between studies. In our study POC production decreased at continuous light while growth rate did not (Figure 4b). While growth rate might be inhibited by a lack of a dark period rather than by photoinhibition (Brand & Guillard, 1981), the decline of POC production at continuous light could partly be due to photoinhibition. Please note (see also above) that the response pattern of CH<sub>4</sub> production is independent of the normalization (cell or POC). Interestingly, it is again CH<sub>4</sub> production that neither levels off nor shows inhibition at continuous light. This observation reinforces the pattern described above, namely, POC production declines while CH<sub>4</sub> production increases further. This “double dependency” of CH<sub>4</sub> production on light, that is, both light intensity and daylength, renders light-dependent processes the prime target for further elucidating the mechanism of CH<sub>4</sub> production in *E. huxleyi*.

## 4.3. Light Intensity Effects on Growth and CH<sub>4</sub> Formation of *E. huxleyi*, *Chrysochromulin* Sp., and *P. globosa*

Methane production was light dependent in *P. globosa* and *Chrysochromulina* sp. too. *Emiliania huxleyi* and *P. globosa* showed a greater light tolerance with respect to growth rate and POC production than *Chrysochromulin* sp. (Figures 5a and 5b). In contrast to POC production and growth rate of *Chrysochromulina* sp., CH<sub>4</sub> production was not inhibited and once again confirms the remarkable light dependency of CH<sub>4</sub> production. The increase in CH<sub>4</sub> production with light intensity in *P. globosa* and *Chrysochromulina* sp. was even higher than that of *E. huxleyi*. However, in each case there was a positive correlation of CH<sub>4</sub> production and light intensity, which could therefore be a common feature of different

phytoplankton taxa. This hypothesis is supported by recent findings of Bižić et al. (2020), who investigated different cyanobacterial species that are found in phytoplankton communities of ocean and lakes. While cyanobacteria produce  $\text{CH}_4$  in light and dark phase, the  $\text{CH}_4$  production rates elevated during the light phase.

#### 4.4. Potential Relevance for $\text{CH}_4$ Production of *E. huxleyi* Populations in the Field

Large blooms of *E. huxleyi* typically occur at subpolar to temperate areas in the summer months, when the water is highly stratified, due to the seasonal increase in temperature and light intensity (Iglesias-Rodríguez et al., 2002; Nanninga & Tyrrell, 1996; Raitso et al., 2006; Tyrrell & Merico, 2004). The occurrence of *E. huxleyi* in field is therefore correlated with high solar radiation, shallow mixed layer depth, and increased sea surface temperature (SST; Raitso et al., 2006). We compare the reported environmental conditions that support *E. huxleyi* growth in the field with those that stimulate  $\text{CH}_4$  production in our laboratory grown cultures to assess whether  $\text{CH}_4$  formation by *E. huxleyi* could be of ecological relevance.

*Emiliania huxleyi* grows at water temperatures between  $1^\circ\text{C}$  and  $31^\circ\text{C}$  in field and has the largest temperature growth range of all *coccolithophores* (McIntyre et al., 1970). The wide temperature range results from the adaptation of individual strains to narrower temperature ranges in cold or warm water masses (Brand, 1982; Langer et al., 2009). The temperature range of the incubation experiments includes the range of the seasonal variation in the SST of the Tasman Sea off New Zealand where the investigated strain (RCC1216) has been isolated and is therefore of ecological relevance. The monthly mean SST of the Tasman Sea off New Zealand ranges from  $13.5^\circ\text{C}$  to  $18.7^\circ\text{C}$  between coldest and warmest month (time period 2007–2017, [https://statistics.shinyapps.io/sea\\_surface\\_temperature\\_oct19/](https://statistics.shinyapps.io/sea_surface_temperature_oct19/), last access: 11 April 2020). With a temperature increase from  $10.1^\circ\text{C}$  to  $21.5^\circ\text{C}$  cellular  $\text{CH}_4$  production rates would double according to laboratory derived rates (section 3.1). Inhibition of growth rate and  $\text{CH}_4$  production due to heat stress is less likely in the field, since the mean SST of the warmest month is below the optimum temperature of the investigated strain. This is in line with literature data showing that most strains grow below their optimal growth condition in field (Langer et al., 2009; Rosas-Navarro et al., 2016).

Our laboratory data also suggest that longer light irradiation periods during summer could have a stimulating effect on  $\text{CH}_4$  production, especially on *E. huxleyi* populations in subpolar regions, where daylength changes dramatically between winter and summer. For example, the  $\text{CH}_4$  production would increase by a factor of 5 due to a daylength increase from 6 hr in winter to 18 hr in summer (section 3.3). *Emiliania huxleyi* usually blooms in the North Atlantic in June and July at high light intensity in the surface layer, which is caused by strong sunlight and shallow mixed layer depth (10–20 m; Nanninga & Tyrrell, 1996; Raitso et al., 2006; Tyrrell & Merico, 2004; Tyrrell & Taylor, 1996). For instance, light intensities of 935 and  $1,140 \mu\text{mol m}^{-2} \text{s}^{-1}$  were measured in *E. huxleyi* blooms in the field. In addition, long-term observations in a mesocosm in a Norwegian fjord have shown that *E. huxleyi* blooms at light intensities between  $>530$  and  $1,200 \mu\text{mol m}^{-2} \text{s}^{-1}$ , whereas the mean light intensities in the surface layer are  $\sim 63\%$  and  $43\%$  of the incident light intensity at 10 and 20 m mixed layer depth, respectively (Nanninga & Tyrrell, 1996, and reference inside). Thus, the *E. huxleyi* cells would have been exposed to light intensities between 228 and  $756 \mu\text{mol m}^{-2} \text{s}^{-1}$  in the mixed layer, which falls within the light intensity range of our incubation experiments (section 3.2). Since the  $\text{CH}_4$  production of *E. huxleyi* increased linearly with the light intensities in culture experiments, the high light intensities in the surface layer could also support the  $\text{CH}_4$  formation of *E. huxleyi* in the field. Judging from our laboratory  $\text{CH}_4$  production and the reported light intensity range where blooms typically occur, the  $\text{CH}_4$  production could vary by a factor of 4. It can be concluded that light intensity will considerably affect sea surface water  $\text{CH}_4$  production of *E. huxleyi* in field.

#### 4.5. The Biogeochemical Perspective: Methane PP ( $\text{CH}_4$ -PP)

While the considerations in section 4.4 apply to the behavior of field populations on the cellular level, they are not appropriate for assessing the biogeochemical significance of this behavior. Several recent studies have emphasized that the PP (see section 2 for calculation), as opposed to the cellular production, is the relevant parameter for biogeochemical assessments (Gafar & Schulz, 2018; Gafar et al., 2018; Klintzsch et al., 2019; Kottmeier et al., 2016; Marra, 2002; Schlüter et al., 2014). We calculated the  $\text{CH}_4$ -PP of *E. huxleyi* for different temperature, light intensity, and daylength conditions. For all three parameters, the  $\text{CH}_4$ -PP increases toward the optimum, as does the cellular  $\text{CH}_4$  production, but the increase in  $\text{CH}_4$ -PP was by 1 order of magnitude higher than for the cellular  $\text{CH}_4$  production (Figures 2c, 3c, and 4c and Figures 2e, 3e,

and 4e). This illustrates the importance of using the PP when considering the biogeochemical impact of changing environmental conditions. Another such illustration is the strong contrast between the light intensity response patterns of cellular, or POC normalized, CH<sub>4</sub> production, and the CH<sub>4</sub>-PP. The sharp decline in CH<sub>4</sub>-PP at the highest light intensity is not reflected in the cellular CH<sub>4</sub> production curve. However, in the field this difference is of minor importance because the highest light intensity used here, ~2,700  $\mu\text{mol m}^{-2} \text{s}^{-1}$ , is considerably higher than even peak light intensities observed in typical *E. huxleyi* blooms (~1,200  $\mu\text{mol m}^{-2} \text{s}^{-1}$ ; see references above). It is noteworthy that the decline in CH<sub>4</sub>-PP at the highest temperature tested here is also of little relevance in the field because *E. huxleyi* usually grows at suboptimal temperatures in the field, a situation that will also not change in the foreseeable future, despite global warming (Rosas-Navarro et al., 2016). It is concluded first that the CH<sub>4</sub>-PP of *E. huxleyi* in the field will be maximal in midsummer when *E. huxleyi* typically blooms. Second, global change will increase the CH<sub>4</sub>-PP of *E. huxleyi* through both warming and increased stratification entailing higher light intensities in the surface layer. Compared to the other two tested haptophytes, *E. huxleyi* has the highest CH<sub>4</sub>-PP, a difference not mirrored in cellular CH<sub>4</sub> production: This is yet another example of the importance of using the PP when considering the biogeochemical impact of CH<sub>4</sub> formation by phytoplankton. As a general caveat it should be noted that the above conclusions are confined to our experimental conditions. Conditions in the field will include other factors such as grazing. This inevitable limitation of experimental data is the price one has to pay for discovering relationships between environmental parameters and the performance of an organism. However, this does not mean that our data are never directly applicable to the field situation as illustrated by the good match of satellite data and *E. huxleyi* calcite production potential reported by Gafar et al. (2018).

## 5. Conclusions

We have determined the CH<sub>4</sub> production of three haptophytes under varying environmental conditions and conclude the following:

1. Temperature, light intensity, and daylength influence CH<sub>4</sub> production.
2. CH<sub>4</sub> production is strongly light dependent; even increasing with light intensity when growth rate and POC production are photoinhibited.
3. The biogeochemically relevant parameter CH<sub>4</sub>-PP increased with temperature, light intensity, and daylength over the range typical for present-day seasonality and global change predictions for the coming century.
4. *E. huxleyi* has a considerably higher CH<sub>4</sub>-PP than *P. globosa* and *Chrysochromulina* sp.

## Conflict of Interest

The authors declare that they have no conflict of interest.

## Data Availability Statement

We provide the data in heiDATA, which is an institutional repository for research data of Heidelberg University (<https://doi.org/10.11588/data/AGKWSG>).

## Acknowledgments

We thank Dr. Markus Greule, Bernd Knape, and Stefan Rheinberger for conducting analytical measurements and for technical support that helped to produce this data set. Furthermore, we are grateful to Dr. Katja Grossmann and Dr. Stefan Schmitt for spectral measurements and Dr. Steffen Greiner for providing microscopy facilities. This work was supported by the Deutsche Forschungsgemeinschaft (Grant Nos. KE 884/11-1 and KE 884/16-2) and the Natural Environment Research Council (NE/N011708/1).

## References

- Balch, W. M., Holligan, P. M., & Kilpatrick, K. A. (1992). Calcification, photosynthesis and growth of the bloom-forming coccolithophore, *Emiliania huxleyi*. *Continental Shelf Research*, 12(12), 1353–1374. [https://doi.org/10.1016/0278-4343\(92\)90059-S](https://doi.org/10.1016/0278-4343(92)90059-S)
- Bange, H. W., & Uher, G. (2005). Photochemical production of methane in natural waters: Implications for its present and past oceanic source. *Chemosphere*, 58(2), 177–183. <https://doi.org/10.1016/j.chemosphere.2004.06.022>
- Bižić, M., Klintzsch, T., Ionescu, D., Hindiyeh, M. Y., Günthel, M., Muro-Pastor, A. M., et al. (2020). Aquatic and terrestrial cyanobacteria produce methane. *Science Advances*, 6(3), eaax5343. <https://doi.org/10.1126/sciadv.aax5343>
- Bogard, M. J., del Giorgio, P. A., Boutet, L., Chaves, M. C. G., Prairie, Y. T., Merante, A., & Derry, A. M. (2014). Oxidic water column methanogenesis as a major component of aquatic CH<sub>4</sub> fluxes. *Nature Communications*, 5(1), 5350. <https://doi.org/10.1038/ncomms6350>
- Bouterfas, R., Belkoura, M., & Dauta, A. (2006). The effects of irradiance and photoperiod on the growth rate of three freshwater green algae isolated from a eutrophic lake. *Limnetica*, 25(3), 647–656.
- Brand, L. E. (1982). Genetic variability and spatial patterns of genetic differentiation in the reproductive rates of the marine coccolithophores *Emiliania huxleyi* and *Gephyrocapsa oceanica* 1,2. *Limnology and Oceanography*, 27(2), 236–245. <https://doi.org/10.4319/lo.1982.27.2.0236>

- Brand, L. E., & Guillard, R. (1981). The effects of continuous light and light intensity on the reproduction rates of twenty-two species of marine phytoplankton. *Journal of Experimental Marine Biology and Ecology*, 50(2–3), 119–132. [https://doi.org/10.1016/0022-0981\(81\)90045-9](https://doi.org/10.1016/0022-0981(81)90045-9)
- Bretherton, L., Poulton, A. J., Lawson, T., Rukminasari, N., Balestreri, C., Schroeder, D., et al. (2019). Day length as a key factor moderating the response of coccolithophore growth to elevated pCO<sub>2</sub>. *Limnology and Oceanography*, 64(3), 1284–1296. <https://doi.org/10.1002/lno.11115>
- Brooks, J. M., Reid, D. F., & Bernard, B. B. (1981). Methane in the upper water column of the northwestern Gulf of Mexico. *Journal of Geophysical Research*, 86(C11), 11,029–11,040. <https://doi.org/10.1029/JC086iC11p11029>
- Brown, C., & Yoder, J. (1994). Distribution pattern of coccolithophorid blooms in the western North Atlantic Ocean. *Continental Shelf Research*, 14(2–3), 175–197. [https://doi.org/10.1016/0278-4343\(94\)90012-4](https://doi.org/10.1016/0278-4343(94)90012-4)
- Burke, R. A. Jr., Reid, D. F., Brooks, J. M., & Lavoie, D. M. (1983). Upper water column methane geochemistry in the eastern tropical North Pacific 1. *Limnology and Oceanography*, 28(1), 19–32. <https://doi.org/10.4319/lno.1983.28.1.0019>
- Conrad, R., & Seiler, W. (1988). Methane and hydrogen in seawater (Atlantic Ocean). *Deep Sea Research Part A: Oceanographic Research Papers*, 35(12), 1903–1917. [https://doi.org/10.1016/0198-0149\(88\)90116-1](https://doi.org/10.1016/0198-0149(88)90116-1)
- Damm, E., Helmke, E., Thoms, S., Schauer, U., Nöthig, E., Bakker, K., & Kiene, R. P. (2010). Methane production in aerobic oligotrophic surface water in the central Arctic Ocean. *Biogeosciences*, 7(3), 1099–1108. <https://doi.org/10.5194/bg-7-1099-2010>
- Damm, E., Kiene, R. P., Schwarz, J., Falck, E., & Dieckmann, G. (2008). Methane cycling in Arctic shelf water and its relationship with phytoplankton biomass and DMSP. *Marine Chemistry*, 109(1–2), 45–59. <https://doi.org/10.1016/j.marchem.2007.12.003>
- de Angelis, M. A., & Lee, C. (1994). Methane production during zooplankton grazing on marine phytoplankton. *Limnology and Oceanography*, 39(6), 1298–1308. <https://doi.org/10.4319/lno.1994.39.6.1298>
- del Valle, D. A., & Karl, D. M. (2014). Aerobic production of methane from dissolved water-column methylphosphonate and sinking particles in the North Pacific Subtropical Gyre. *Aquatic Microbial Ecology*, 73(2), 93–105. <https://doi.org/10.3354/ame01714>
- DeLong, J. P., Gibert, J. P., Lühring, T. M., Bachman, G., Reed, B., Neyer, A., & Montooth, K. L. (2017). The combined effects of reactant kinetics and enzyme stability explain the temperature dependence of metabolic rates. *Ecology and Evolution*, 7(11), 3940–3950. <https://doi.org/10.1002/ece3.2955>
- Edwards, K. F., Thomas, M. K., Klausmeier, C. A., & Litchman, E. (2015). Light and growth in marine phytoplankton: Allometric, taxonomic, and environmental variation. *Limnology and Oceanography*, 60(2), 540–552. <https://doi.org/10.1002/lno.10033>
- Florez-Leiva, L., Damm, E., & Farias, L. (2013). Methane production induced by dimethylsulfide in surface water of an upwelling ecosystem. *Progress in Oceanography*, 112, 38–48.
- Forster, G., Upstill-Goddard, R. C., Gist, N., Robinson, C., Uher, G., & Woodward, E. M. S. (2009). Nitrous oxide and methane in the Atlantic Ocean between 50°N and 52°S: Latitudinal distribution and sea-to-air flux. *Deep Sea Research Part II: Topical Studies in Oceanography*, 56(15), 964–976. <https://doi.org/10.1016/j.dsr2.2008.12.002>
- Gafar, N. A., Eyre, B. D., & Schulz, K. G. (2018). A conceptual model for projecting coccolithophorid growth, calcification and photosynthetic carbon fixation rates in response to global ocean change. *Frontiers in Marine Science*, 4, 433. <https://doi.org/10.3389/fmars.2017.00433>
- Gafar, N. A., & Schulz, K. G. (2018). A three-dimensional niche comparison of *Emiliania huxleyi* and *Gephyrocapsa oceanica*: Reconciling observations with projections. *Biogeosciences*, 15(11), 3541–3560. <https://doi.org/10.5194/bg-15-3541-2018>
- Ghyczy, M., Torday, C., Kaszaki, J., Szabo, A., Czobél, M., & Boros, M. (2008). Hypoxia-induced generation of methane in mitochondria and eukaryotic cells—An alternative approach to methanogenesis. *Cellular Physiology and Biochemistry*, 21(1–3), 251–258. <https://doi.org/10.1159/000113766>
- Gillooly, J. F., Brown, J. H., West, G. B., Savage, V. M., & Charnov, E. L. (2001). Effects of size and temperature on metabolic rate. *Science*, 293(5538), 2248–2251. <https://doi.org/10.1126/science.1061967>
- Glover, H. E., Keller, M. D., & Spinrad, R. W. (1987). The effects of light quality and intensity on photosynthesis and growth of marine eukaryotic and prokaryotic phytoplankton clones. *Journal of Experimental Marine Biology and Ecology*, 105(2–3), 137–159. [https://doi.org/10.1016/0022-0981\(87\)90168-7](https://doi.org/10.1016/0022-0981(87)90168-7)
- Grimaud, G. M., Mairet, F., Sciandra, A., & Bernard, O. (2017). Modeling the temperature effect on the specific growth rate of phytoplankton: A review. *Reviews in Environmental Science and Bio/Technology*, 16(4), 625–645. <https://doi.org/10.1007/s11157-017-9443-0>
- Grossart, H.-P., Frindt, K., Dzallas, C., Eckert, W., & Tang, K. W. (2011). Microbial methane production in oxygenated water column of an oligotrophic lake. *Proceedings of the National Academy of Sciences*, 108(49), 19,657–19,661. <https://doi.org/10.1073/pnas.1110716108>
- Guillard, R. R., & Ryther, J. H. (1962). Studies of marine planktonic diatoms: I. *Cyclotella nana* Hustedt, and *Detonula confervacea* (Cleve) Gran. *Canadian Journal of Microbiology*, 8(2), 229–239. <https://doi.org/10.1139/m62-029>
- Günthel, M., Donis, D., Kirillin, G., Ionescu, D., Bizic, M., McGinnis, D. F., et al. (2019). Contribution of oxic methane production to surface methane emission in lakes and its global importance. *Nature Communications*, 10(1), 5497. <https://doi.org/10.1038/s41467-019-13320-0>
- Harris, G. N., Scanlan, D. J., & Geider, R. J. (2005). Acclimation of *Emiliania huxleyi* (Prymnesiophyceae) to photon flux density. *Journal of Phycology*, 41(4), 851–862. <https://doi.org/10.1111/j.1529-8817.2005.00109.x>
- Hartmann, J. F., Günthel, M., Klintzsch, T., Kirillin, G., Grossart, H.-P., Keppler, F., & Isenbeck-Schröter, M. (2020). High spatiotemporal dynamics of methane production and emission in oxic surface water. *Environmental Science & Technology*, 54(3), 1451–1463. <https://doi.org/10.1021/acs.est.9b03182>
- Iglesias-Rodríguez, M. D., Brown, C. W., Doney, S. C., Kleypas, J., Kolber, D., Kolber, Z., et al. (2002). Representing key phytoplankton functional groups in ocean carbon cycle models: Coccolithophorids. *Global Biogeochemical Cycles*, 16(4), 1100. <https://doi.org/10.1029/2001GB001454>
- Jugold, A., Althoff, F., Hurkuck, M., Greule, M., Lenhart, K., Lelieveld, J., & Keppler, F. (2012). Non-microbial methane formation in oxic soils. *Biogeosciences*, 9(12), 5291–5301. <https://doi.org/10.5194/bg-9-5291-2012>
- Karl, D. M., Beversdorf, L., Bjorkman, K. M., Church, M. J., Martinez, A., & DeLong, E. F. (2008). Aerobic production of methane in the sea. *Nature Geoscience*, 1(7), 473–478. <https://doi.org/10.1038/ngeo234>
- Karl, D. M., & Tilbrook, B. D. (1994). Production and transport of methane in oceanic particulate organic matter. *Nature*, 368(6473), 732–734. <https://doi.org/10.1038/368732a0>
- Keppler, F., Hamilton, J. T., Braß, M., & Röckmann, T. (2006). Methane emissions from terrestrial plants under aerobic conditions. *Nature*, 439(7073), 187–191. <https://doi.org/10.1038/nature04420>
- Keppler, F., Schiller, A., Ehehalt, R., Greule, M., Hartmann, J., & Polag, D. (2016). Stable isotope and high precision concentration measurements confirm that all humans produce and exhale methane. *Journal of Breath Research*, 10(1), 016003. <https://doi.org/10.1088/1752-7155/10/1/016003/pdf>

- Kingsolver, J. G. (2009). The well-temperated biologist. (American Society of Naturalists Presidential Address). *The American Naturalist*, 174(6), 755–768. <https://doi.org/10.1086/648310>
- Kirschke, S., Bousquet, P., Ciais, P., Saunio, M., Canadell, J. G., Dlugokencky, E. J., et al. (2013). Three decades of global methane sources and sinks. *Nature Geoscience*, 6(10), 813–823. <https://doi.org/10.1038/ngeo1955>
- Klitzsch, T., Langer, G., Nehrke, G., Wieland, A., Lenhart, K., & Keppler, F. (2019). Methane production by three widespread marine phytoplankton species: Release rates, precursor compounds, and potential relevance for the environment. *Biogeosciences*, 16(20), 4129–4144. <https://doi.org/10.5194/bg-16-4129-2019>
- Kottmeier, D. M., Rokitta, S. D., & Rost, B. (2016). H<sup>+</sup>-driven increase in CO<sub>2</sub> uptake and decrease in uptake explain coccolithophores' acclimation responses to ocean acidification. *Limnology and Oceanography*, 61(6), 2045–2057. <https://doi.org/10.1002/lno.10352>
- Lamontagne, R. A., Smith, W. D., & Swinnerton, J. W. (1975). C1–C3 hydrocarbons and chlorophyll a concentrations in the equatorial Pacific Ocean. In *Analytical Methods in Oceanography* (Vol. 147, pp. 163–171). Washington, DC: American Chemical Society.
- Langer, G., Nehrke, G., Probert, I., Ly, J., & Ziveri, P. (2009). Strain-specific responses of *Emiliania huxleyi* to changing seawater carbonate chemistry. *Biogeosciences*, 6(11), 2637–2646. <https://doi.org/10.5194/bg-6-2637-2009>
- Langer, G., Oetjen, K., & Brenneis, T. (2012). Calcification of *Calcidiscus leptoporus* under nitrogen and phosphorus limitation. *Journal of Experimental Marine Biology and Ecology*, 413, 131–137. <https://doi.org/10.1016/j.jembe.2011.11.028>
- Langer, G., Oetjen, K., & Brenneis, T. (2013). Coccolithophores do not increase particulate carbon production under nutrient limitation: A case study using *Emiliania huxleyi* (PML B92/11). *Journal of Experimental Marine Biology and Ecology*, 443, 155–161. <https://doi.org/10.1016/j.jembe.2013.02.040>
- Lenhart, K., Bunge, M., Ratering, S., Neu, T. R., Schüttmann, I., Greule, M., et al. (2012). Evidence for methane production by saprotrophic fungi. *Nature Communications*, 3(1), 1046. <https://doi.org/10.1038/ncomms2049>
- Lenhart, K., Klitzsch, T., Langer, G., Nehrke, G., Bunge, M., Schnell, S., & Keppler, F. (2016). Evidence for methane production by the marine algae *Emiliania huxleyi*. *Biogeosciences*, 13(10), 3163–3174. <https://doi.org/10.5194/bg-13-3163-2016>
- Lenhart, K., Weber, B., Elbert, W., Steinkamp, J., Clough, T., Crutzen, P., et al. (2015). Nitrous oxide and methane emissions from cryptogamic covers. *Global Change Biology*, 21(10), 3889–3900. <https://doi.org/10.1111/gcb.12995>
- Liu, J., Hartmann, S. C., Keppler, F., & Lai, D. Y. F. (2019). Simultaneous abiotic production of greenhouse gases (CO<sub>2</sub>, CH<sub>4</sub>, and N<sub>2</sub>O) in subtropical soils. *Journal of Geophysical Research: Biogeosciences*, 124, 1977–1987. <https://doi.org/10.1029/2019JG005154>
- Loebl, M., Cockshutt, A. M., Campbell, D. A., & Finkel, A. Z. V. (2010). Physiological basis for high resistance to photoinhibition under nitrogen depletion in *Emiliania huxleyi*. *Limnology and Oceanography*, 55(5), 2150–2160. <https://doi.org/10.4319/lno.2010.55.5.2150>
- Marra, J. (2002). Approaches to the measurement of plankton production. *Phytoplankton productivity: Carbon assimilation in marine and freshwater ecosystems*, 78–108. <https://doi.org/10.1002/9780470995204.ch4>
- McIntyre, A., Bé, A. W., & Roche, M. B. (1970). Modern Pacific Coccolithophorida: A paleontological thermometer. *Transactions of the New York Academy of Sciences*, 32(6 Series II), 720–731. <https://doi.org/10.1111/j.2164-0947.1970.tb02746.x>
- Menden-Deuer, S., & Lessard, E. J. (2000). Carbon to volume relationships for dinoflagellates, diatoms, and other protist plankton. *Limnology and Oceanography*, 45(3), 569–579. <https://doi.org/10.4319/lno.2000.45.3.0569>
- Metcalfe, W. W., Griffin, B. M., Cicchillo, R. M., Gao, J., Janga, S. C., Cooke, H. A., et al. (2012). Synthesis of methylphosphonic acid by marine microbes: A source for methane in the Aerobic Ocean. *Science*, 337(6098), 1104–1107. <https://doi.org/10.1126/science.1219875>
- Nanninga, H., & Tyrrell, T. (1996). Importance of light for the formation of algal blooms by *Emiliania huxleyi*. *Marine Ecology Progress Series*, 136, 195–203. <https://doi.org/10.3354/meps136195>
- Nielsen, M. V. (1997). Growth, dark respiration and photosynthetic parameters of the coccolithophorid *Emiliania huxleyi* (Prymnesiophyceae) acclimated to different day length-irradiance combinations. *Journal of Phycology*, 33(5), 818–822. <https://doi.org/10.1111/j.0022-3646.1997.00818.x>
- Olenina, I., Hajdu, S., Edler, L., Andersson, A., Wasmund, N., Busch, S., et al. (2006). *Biovolumes and size-classes of phytoplankton in the Baltic Sea* (pp. 1–144). Paper presented at HELCOM Baltic Sea Environment Proceedings No. 106.
- Oudot, C., Jean-Baptiste, P., Fourré, E., Mormiche, C., Guevel, M., Terner, J.-F., & le Corre, P. (2002). Transatlantic equatorial distribution of nitrous oxide and methane. *Deep Sea Research Part I: Oceanographic Research Papers*, 49(7), 1175–1193. [https://doi.org/10.1016/S0967-0637\(02\)00019-5](https://doi.org/10.1016/S0967-0637(02)00019-5)
- Owens, N. J. P., Law, C. S., Mantoura, R. F. C., Burkill, P. H., & Llewellyn, C. A. (1991). Methane flux to the atmosphere from the Arabian Sea. *Nature*, 354(6351), 293–296. <https://doi.org/10.1038/354293a0>
- Paasche, E. (1967). Marine plankton algae grown with light-dark cycles. I. *Coccolithus huxleyi*. *Physiologia Plantarum*, 20(4), 946–956. <https://doi.org/10.1111/j.1399-3054.1967.tb08382.x>
- Raitos, D. E., Lavender, S. J., Pradhan, Y., Tyrrell, T., Reid, P. C., & Edwards, M. (2006). Coccolithophore bloom size variation in response to the regional environment of the subarctic North Atlantic. *Limnology and Oceanography*, 51(5), 2122–2130. <https://doi.org/10.4319/lno.2006.51.5.2122>
- Rakowski, C., Magen, C., Bosman, S., Gillies, L., Rogers, K., Chanton, J., & Mason, O. U. (2015). Methane and microbial dynamics in the Gulf of Mexico water column. *Frontiers in Marine Science*, 2, 69.
- Repet, D. J., Ferrón, S., Sosa, O. A., Johnson, C. G., Repet, L. D., Acker, M., et al. (2016). Marine methane paradox explained by bacterial degradation of dissolved organic matter. *Nature Geoscience*, 9(12), 884–887. <https://doi.org/10.1038/ngeo2837>
- Rosas-Navarro, A., Langer, G., & Ziveri, P. (2016). Temperature affects the morphology and calcification of *Emiliania huxleyi* strains. *Biogeosciences*, 13(10), 2913–2926. <https://doi.org/10.5194/bg-13-2913-2016>
- Saunio, M., Bousquet, P., Poulter, B., Peregón, A., Ciais, P., Canadell, J. G., et al. (2016). The global methane budget 2000–2012. *Earth System Science Data*, 8(2), 697–751. <https://doi.org/10.5194/essd-8-697-2016>
- Schindelin, J., Arganda-Carreras, I., Frise, E., Kaynig, V., Longair, M., Pietzsch, T., et al. (2012). Fiji: An open-source platform for biological-image analysis. *Nature Methods*, 9(7), 676–682. <https://doi.org/10.1038/nmeth.2019>
- Schlüter, L., Lohbeck, K. T., Gutowska, M. A., Gröger, J. P., Riebesell, U., & Reusch, T. B. H. (2014). Adaptation of a globally important coccolithophore to ocean warming and acidification. *Nature Climate Change*, 4(11), 1024–1030. <https://doi.org/10.1038/nclimate2379>
- Schmale, O., Wäge, J., Mohrholz, V., Wasmund, N., Gräwe, U., Rehder, G., et al. (2018). The contribution of zooplankton to methane supersaturation in the oxygenated upper waters of the central Baltic Sea. *Limnology and Oceanography*, 63(1), 412–430. <https://doi.org/10.1002/lno.10640>
- Schoemann, V., Becquevort, S., Stefels, J., Rousseau, V., & Lancelot, C. (2005). Phaeocystis blooms in the global ocean and their controlling mechanisms: A review. *Journal of Sea Research*, 53(1–2), 43–66. <https://doi.org/10.1016/j.seares.2004.01.008>
- Scranton, M. I. (1977). *The marine geochemistry of methane* (PhD thesis, pp. 1–251). Massachusetts, USA: Institute of Technology and Woods Hole Oceanographic Institution.

- Scranton, M. I., & Brewer, P. G. (1977). Occurrence of methane in the near-surface waters of the western subtropical North-Atlantic. *Deep Sea Research*, 24(2), 127–138.
- Scranton, M. I., & Farrington, J. W. (1977). Methane production in the waters off Walvis Bay. *Journal of Geophysical Research*, 82(31), 4947–4953. <https://doi.org/10.1029/JC082i031p04947>
- Segel, I. H. (1993). *Enzyme kinetics: Behavior and analysis of rapid equilibrium and steady-state enzyme systems*. New York: John Wiley & Sons.
- Stawiarski, B., Otto, S., Thiel, V., Gräwe, U., Loick-Wilde, N., Wittenborn, A. K., et al. (2019). Controls on zooplankton methane production in the central Baltic Sea. *Biogeosciences*, 16(1), 1–16. <https://doi.org/10.5194/bg-16-1-2019>
- Tang, K. W., McGinnis, D. F., Frindte, K., Brüchert, V., & Grossart, H.-P. (2014). Paradox reconsidered: Methane oversaturation in well-oxygenated lake waters. *Limnology and Oceanography*, 59(1), 275–284. <https://doi.org/10.4319/lo.2014.59.1.0275>
- Tang, K. W., McGinnis, D. F., Ionescu, D., & Grossart, H.-P. (2016). Methane production in oxic lake waters potentially increases aquatic methane flux to air. *Environmental Science & Technology Letters*, 3(6), 227–233. <https://doi.org/10.1021/acs.estlett.6b00150>
- Thauer, R. K., Kaster, A. K., Seedorf, H., Buckel, W., & Hedderich, R. (2008). Methanogenic archaea: Ecologically relevant differences in energy conservation. *Nature Reviews. Microbiology*, 6(8), 579–591. <https://doi.org/10.1038/nrmicro1931>
- Thomsen, H. A. (1994). 10. Haptophytes as components of marine phytoplankton. Haptophytes as components of marine phytoplankton. In *The Haptophyte Algae*, B. S. C. (pp. 187–208). Oxford: Clarendon Press.
- Trimborn, S., Langer, G., & Rost, B. r. (2007). Effect of varying calcium concentrations and light intensities on calcification and photosynthesis in *Emiliania huxleyi*. *Limnology and Oceanography*, 52(5), 2285–2293. <https://doi.org/10.4319/lo.2007.52.5.2285>
- Tyrrell, T., & Merico, A. (2004). *Emiliania huxleyi*: Bloom observations and the conditions that induce them. In *Coccolithophores* (pp. 75–97). New York: Springer.
- Tyrrell, T., & Taylor, A. (1996). A modelling study of *Emiliania huxleyi* in the NE Atlantic. *Journal of Marine Systems*, 9(1–2), 83–112. [https://doi.org/10.1016/0924-7963\(96\)00019-X](https://doi.org/10.1016/0924-7963(96)00019-X)
- Van Rijssel, M., & Gieskes, W. W. (2002). Temperature, light, and the dimethylsulfoniopropionate (DMSP) content of *Emiliania huxleyi* (Prymnesiophyceae). *Journal of Sea Research*, 48(1), 17–27. [https://doi.org/10.1016/S1385-1101\(02\)00134-X](https://doi.org/10.1016/S1385-1101(02)00134-X)
- Watanabe, S., Higashitani, N., Tsurushima, N., & Tsunogai, S. (1995). Methane in the western North Pacific. *Journal of Oceanography*, 51(1), 39–60. <https://doi.org/10.1007/BF02235935>
- Weber, T., Wiseman, N. A., & Kock, A. (2019). Global ocean methane emissions dominated by shallow coastal waters. *Nature Communications*, 10(1), 4584. <https://doi.org/10.1038/s41467-019-12541-7>
- Weller, D. I., Law, C. S., Marriner, A., Nodder, S. D., Chang, F. H., Stephens, J. A., et al. (2013). Temporal variation of dissolved methane in a subtropical mesoscale eddy during a phytoplankton bloom in the southwest Pacific Ocean. *Progress in Oceanography*, 116, 193–206. <https://doi.org/10.1016/j.pocean.2013.07.008>
- Wiesenburg, D. A., & Guinasso, N. L. (1979). Equilibrium solubilities of methane, carbon monoxide, and hydrogen in water and sea water. *Journal of Chemical & Engineering Data*, 24(4), 356–360. <https://doi.org/10.1021/je60083a006>
- Zhang, Y., Bach, L. T., Schulz, K. G., & Riebesell, U. (2015). The modulating effect of light intensity on the response of the coccolithophore *Gephyrocapsa oceanica* to ocean acidification. *Limnology and Oceanography*, 60(6), 2145–2157. <https://doi.org/10.1002/lno.10161>
- Zhang, Y., & Xie, H. (2015). Photomineralization and photomethanification of dissolved organic matter in Saguenay River surface water. *Biogeosciences*, 12(22), 6823–6836. <https://doi.org/10.5194/bg-12-6823-2015>
- Zindler, C., Bracher, A., Marandino, C. A., Taylor, B., Torrecilla, E., Kock, A., & Bange, H. W. (2013). Sulphur compounds, methane, and phytoplankton: Interactions along a north-south transit in the western Pacific Ocean. *Biogeosciences*, 10(5), 3297–3311. <https://doi.org/10.5194/bg-10-3297-2013>